New Discretization Procedure for the Breakage Equation

Priscilla J. Hill and Ka M. Ng
Dept. of Chemical Engineering, University of Massachusetts, Amherst, MA 01003

A new discretization method, applicable for both batch and continuous systems, is developed for the breakage equation. The problem of intrainterval interactions due to discretization is accounted for by matching the zeroth and first moments of the continuous population balance equation with the corresponding moments of the discretized equation, thereby guaranteeing conservation of mass and total number of particles. Without loss of generality, the use of this method is demonstrated with a power law form of the specific rate of breakage, and with both theoretical and empirical breakage functions. The systematic method requires minimum computational efforts by allowing the user to choose either geometric size intervals with any geometric ratio or equal-size intervals for the particle size range. Simulation results show that the new method significantly improves predictions of the particle size distribution over the discretization method currently in use.

Introduction

Population balance equations (PBEs) are used in a number of diverse fields such as atmospheric science, crystallization, and comminution, for materials ranging from aerosols, emulsions, dispersions, cell populations, and crystals. Recently, these equations are also used in computer-aided simulation of processes containing solids processing steps; examples of solids plants include the production of potash, ammonium sulfate, citric acid, alumina, titanium dioxide, adipic acid, supported catalysts, and plants for coal and hydrometallurgical processes. The impetus for using PBEs is the desire to follow the evolution of the particle size distribution (PSD) from one equipment unit to another, which is essential for process design and optimization (Neville and Seider, 1980; Jones, 1984; Barton and Perkins, 1988; Evans, 1989; Rajagopal et al., 1988, 1992). A generic form of PBEs is:

$$\frac{d}{dt}n(z,t;v) = [\text{accumulation}]$$

$$= [\text{inflow}] - [\text{outflow}] + [\text{birth}] - [\text{death}]. \quad (1)$$

Here, the dependent variable, $n(z,t;v)\,dv$, is the number concentration of particles having volumes between v and $v+dv$ at position z and time t. The inflow (outflow) term accounts for the addition (removal) of particles to (from) the system. The birth term represents an increase in the number of particles due to nucleation, growth, dissolution, agglomeration, and/or breakage. Similarly, the death term represents a reduction in the number of particles due to growth, dissolution, agglomeration, and/or breakage. Different forms of Eq. 1 are used for different equipment units. For example, a batch crusher generally requires only two terms on the righthand side (RHS) of Eq. 1, a birth term due to the breakage of large particles to form particles of volume v and a death term accounting for the disappearance of the particles of volume v due to breakage. We will focus in this article on this special form of PBE, referred to as the *breakage equation*. However, the discussions are equally valid for a system with inflow and outflow.

The number density function, $n(v)$, in Eq. 1 changes continuously with the particle size. Thus, it represents a *continuous PSD* and should be used in a *continuous PBE*. In contrast, a *discretized PSD*, in which the particle size range is divided into a number of size intervals, is used in a *discretized PBE*. Only a single value N_i is specified for the number of particles per unit volume of slurry or per unit mass of powder within a given size interval i.

Recent developments indicate that discretized PBEs are the ones to use in process synthesis and simulation (Goldfarb et al., 1990). There are three main reasons for this trend. The

Correspondence concerning this article should be addressed to K. M. Ng.

first is a practical one. Despite the fact that modern instruments, such as the various laser-light-diffraction techniques (e.g., Lasentec), can be used to measure an essentially continuous PSD, such plant data are not yet generally available. Instead, it is more common to have data similar to those obtained in sieve analysis of a powder; that is, only a limited number of intervals, on the order of ten to twenty, are used to cover the entire size range. The second reason for choosing discretized PBEs for process simulation is that the discretized PSD fits in much better with the data structure used in large-scale simulation codes (Evans et al., 1977). With the exception of the standard continuous distributions such as the Gaussian, Rosin-Rammler, and log-normal, it is easier to store an arbitrary PSD in discretized form in the computer program. The third reason is that once discretized, the population balance is a set of differential equations for $N_i(z,t)$. Without the explicit dependence on size, these equations can be integrated in a routine manner.

However, solutions of the discretized PBEs are not without problems. The continuous PBE is fundamentally exact, in that the particle density function $n(z,t;v)$ reflects the fact that it is actually a continuous function for a large population of particles. A common question in the solution of discretized PBEs, therefore, is how do we know that the number of size intervals is sufficient to predict an answer close to, and preferably identical to, that obtained from the fundamentally exact continuous PBEs? The current practice is to increase the number of size intervals. If the predicted PSD remains approximately the same as the number of size intervals increases, the answer is believed to be acceptable. A review of solutions to discretized PBEs shows that as many as 600 size intervals were used (Gelbard, 1979). This approach is very tedious indeed.

In addition, there is a more fundamental problem in the use of discretized PBEs. The underlying difficulty is that no matter how small a size interval is, in addition to interinterval particle interactions, particles within a given interval actually still interact with one another. As a result, loss or generation of particles due to discretization cannot be prevented at long times. We will explain this point in more detail below.

Thus, the aim of this article is to develop a systematic method for the use of discretized PBEs in the simulation of breakage processes. It has the following attributes:

- It provides an output discretized PSD that is guaranteed to have the same or nearly the same zeroth moment (total number of particles) and first moment (total mass of particles) as that obtained from an exact solution of the fundamentally exact continuous PBE.
- The number and range of size intervals can be specified by the user without compromising the attribute just stated. For particulate systems, the use of equal-sized intervals is often not the optimal choice. For example, the log normal distribution has very few large particles at the high end of the distribution function. To reduce the number of computations, it is more advantageous to divide up the particle-size domain such that the sizes of the intervals are in a geometric series: $v_{i+1} = rv_i$, where r is the geometric ratio and v_i is the largest size for interval i.
- It is capable of simulating the experimental data of solids processing units such as crushers and grinders.

Literature Review

Solution of population balance equations

A discussion of the existing solution methods as well as a comprehensive listing of the relevant references for the different methods is given in a review on PBEs by Ramkrishna (1985). It was pointed out that analytical solutions to PBEs can be found only in a number of simplified cases and that numerical solutions are often needed. The different methods include: method of moments (Hulburt and Katz, 1964), transform techniques (Ramabhadran et al., 1976), method of weighted residuals (Ramkrishna, 1971), approximation techniques (Cohen and Vaughan, 1971), similarity solutions (Ramabhadran and Seinfeld, 1975), Monte Carlo simulations (Shah et al., 1977), among others. The existence of steady-state solutions to PBEs was considered by Vigil and Ziff (1989). All of the preceding are intended for continuous PBEs. For discretized breakage equations, a number of analytical solutions are available for a batch system (Ziff and McGrady, 1985; Ziff, 1991, 1992) and for a system with inflow and outflow of particles (McGrady and Ziff, 1988).

The most relevant recent development on solving discretized PBEs is due to Hounslow et al. (1988) and Hounslow (1990). They considered a crystallizer with nucleation, growth, and coalescence, *but no breakage*. They suggested a new method to formulate the discretized PBE in such a way that the zeroth and first moments obtained with the discretized PBE match the corresponding moments obtained with the continuous PBE. However, the method for coalescence is limited to the case where the sizes of the intervals are in a geometric series $v_{i+1} = 2v_i$: the geometric ratio is limited to 2. Conservation of the number and volume of particles is similarly achieved in our work on the breakage equation.

Review of the breakage equation

The breakage equation for a batch system has been presented in the literature in a number of forms, which can be a source of confusion. For clarity, a brief review of the four major forms as well as some relevant relations is given below. It is a continuous (discretized) equation when $n(v)$ (N_i) is used, and it can be either mass-based or number-based.

Mass-Based Breakage Equation. The *continuous mass-based breakage equation* is used primarily in the area of crushing and grinding (Prasher, 1987):

$$\frac{d}{dt}M(v,t) = \int_v^\infty S_M(w)b_M(v,w)M(w,t)dw - S_M(v)M(v,t). \quad (2)$$

It states that the rate of change of the mass of particles between volumes v and $v+dv$, $M(v)\,dv$, is the net result of generation due to breakage of particles larger than v and loss of particles of size v by breakage into smaller sizes. The specific rate of breakage, $S_M(v)$, is the mass fraction of particles of volume v broken per unit time. The breakage function, $b_M(v,w)\,dv$, is the mass fraction of particles, broken from volume w, that fall into the volume range v to $v+dv$. To conserve mass, all of the mass fractions formed must sum to unity. Thus, we have

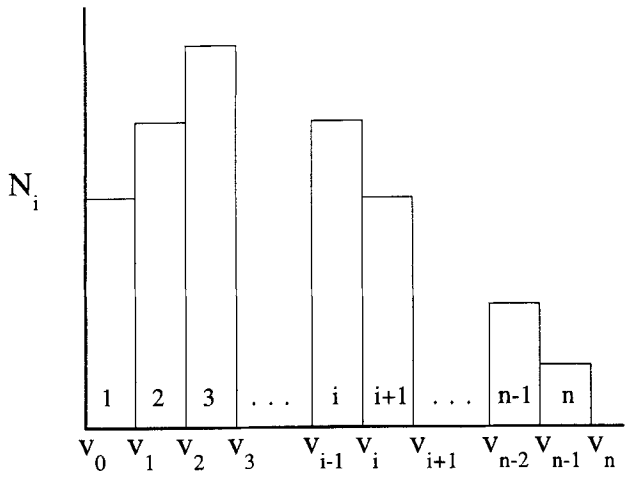

Figure 1. Numbering system for discretized intervals.

$$\int_0^w b_M(v,w)\,dv = 1. \tag{3}$$

Instead of $b_M(v,w)$, the cumulative breakage function, $B_M(v,w)$, is frequently used to correlate experimental data on breakage in the literature. It represents the mass fraction of particles, broken from volume w, that are smaller than or equal to volume v. The relation between $B_M(v,w)$ and $b_M(v,w)$ is given by

$$B_M(v,w) = \int_0^v b_M(v',w)\,dv', \tag{4}$$

where v' is a dummy volume.

The discretized counterpart of Eq. 2, the *discretized mass-based breakage equation*, is often expressed as the following:

$$\frac{d\omega_i}{dt} = \sum_{j=i+1}^{\infty} b_{Mij} S_{Mj} \omega_j - S_{Mi}\omega_i. \tag{5}$$

As shown in Figure 1, the intervals are numbered consecutively from small to large sizes with interval i containing particles larger than v_{i-1} and smaller than or equal to v_i. For the first interval, v_0 is equal to zero. In the crushing and grinding literature, intervals are often numbered from large to small sizes. The discretized mass-based breakage function, b_{Mij}, is the mass fraction of particles broken from interval j that fall into interval i. This discretized function is related to the continuous cumulative breakage function by

$$b_{Mij} = [B_M(v_i, v_{j-1}) - B_M(v_{i-1}, v_{j-1})]. \tag{6}$$

The following constraint is often assumed in the literature for the discretized breakage function:

$$\sum_{i=1}^{j-1} b_{Mij} = 1. \tag{7}$$

In other words, it assumes that none of the particles broken from interval j would form particles in interval j or that b_{Mjj} is zero. The analog of Eq. 4 is

$$B_{Mij} = \sum_{k=1}^{i} b_{Mkj}. \tag{8}$$

It is the mass fraction of particles broken from interval j that fall into an interval less than or equal to interval i.

Number-Based Breakage Equation. The particle density function, $n(v)$, is used in the *continuous number-based breakage equation* below:

$$\frac{dn(v)}{dt} = \int_v^{\infty} b(v,w) S(w) n(w)\,dw - S(v)n(v). \tag{9}$$

While the mass-based breakage equation is used for crushing and grinding, the number-based equation is the form used in describing other solids processing operations (Randolph and Larson, 1988). For example, PBEs for modeling crystallizer performance are number-based. The number-based specific rate of breakage, $S(v)$, is the number fraction of particles broken from volume v per unit time. Multiplying and dividing $S_M(v)$ by the particle density, it can be shown that

$$S(v) = S_M(v). \tag{10}$$

The number-based breakage function, $b(v,w)\,dv$, is the number of particles formed between v and $v + dv$ divided by the number of particles broken from volume w. The number- and mass-based breakage functions are related by the following relation:

$$b(v,w) = \frac{w}{v} b_M(v,w). \tag{11}$$

While the mass-based breakage function should always be less than or equal to unity, the number-based breakage function can be greater than unity. Specifically, if each particle that is broken forms m smaller particles, then the number-based breakage function is constrained by the following equation:

$$\int_0^w b(v,w)\,dv = m. \tag{12}$$

Let us focus on binary breakage, that is, m equals 2. In this case, the breakage function is constrained by the following symmetry requirement:

$$b(v,w) = b(w - v, w). \tag{13}$$

The *discretized number-based breakage equation* is often expressed as follows:

$$\frac{d}{dt}N_i(t) = \sum_{j=i+1}^{\infty} b_{ij} S_j N_j(t) - S_i N_i(t). \tag{14}$$

Because of Eq. 10, the specific rate of breakage, S_i, is the same as S_{Mi} in Eq. 5. The number-based breakage function, b_{ij}, is the number of child particles that fall in interval i from the breakage of one particle in interval j. Analogous to Eq. 6, the following relation holds:

$$b_{ij} = [B(v_i, v_{j-1}) - B(v_{i-1}, v_{j-1})]. \tag{15}$$

Here, B is the number-based counterpart of B_M in Eq. 4; that is,

$$B(v,w) = \int_0^v b(v',w)\, dv', \tag{16}$$

where v' is a dummy volume. As in Eq. 7, the following constraint for binary breakage is often assumed:

$$\sum_{i=1}^{j-1} b_{ij} = 2. \tag{17}$$

Equation 17 assumes that particles broken from interval j cannot fall back into the same interval. Similar to Eq. 8, a discretized number-based cumulative breakage function can also be defined:

$$B_{ij} = \sum_{k=1}^{i} b_{kj}. \tag{18}$$

Furthermore, since moments are frequently used in describing a PSD, the following definitions are needed at a later stage. The jth moment of the number density function is defined as

$$m_j = \int_0^\infty v^j n(v)\, dv. \tag{19}$$

For discretized equations, the jth moment is calculated using the following expression:

$$m_j = \sum_{i=1}^{\infty} \bar{v}_i^j N_i. \tag{20}$$

Here, $\bar{v}_i$ is any representative size for interval i. In this article, the arithmetic mean is chosen for use in our calculations; that is,

$$\bar{v}_i = \frac{v_i + v_{i-1}}{2}. \tag{21}$$

Functional Forms for $S(v)$ and $b(v,w)$. Experimental data indicate that $S_M(v)$ can be generally represented as a power law form. However, when particles are crushed or ground below a critical size, plasticity sets in and further breakage ceases (Kendall, 1978; Prasher, 1987). The value of the critical size depends on the material properties and the type of machine under consideration. Therefore, we assume that the rate of breakage for particles of size less than v_1 is zero. Thus, for $v < v_1$ we have

$$S(v) = 0 \tag{22}$$

and for $v \geq v_1$ we have

$$S(v) = S_c v^\alpha. \tag{23}$$

Here, S_c is a constant and α is nonnegative. In the event that the breakage rate is independent of particle size, α equals zero in Eq. 23 and we have

$$S(v) = S_c. \tag{24}$$

Intrinsic problem of intrainterval interactions

To qualitatively understand the intrainterval interactions problem, let us consider the following hypothetical example for binary breakage. Particles of volume ranging from 0 to 10 mm^3 are arbitrarily divided up into four intervals—0 to 1, 1 to 3, 3 to 5, and 5 to 10. Focus on the last term of Eq. 14 and the last size interval, 5 to 10 mm^3. When a particle in this size interval breaks, for example, a 7-mm^3 particle, it can break into a 6-mm^3 plus a 1-mm^3 particle; a 5 plus a 2, and a 4 plus a 3, as well as all other fractional sizes. It is sufficient to consider only the integral sizes to demonstrate the existence of the intrinsic problem. When a 7-mm^3 particle breaks into a 6 plus a 1, the number of particles in the last interval, N_4, is automatically reduced by 1 with the discretized breakage equation. Actually, N_4 does not decrease because the newly created particle of volume 6 mm^3 belongs to the same interval, that is, from 5 to 10 mm^3. The net change in N_4 should have been nil. The result is that the conventional number-based discretized PBE (Eq. 14) predicts a value for the total number of particles different from the exact answer of the continuous PBE (Eq. 9).

As mentioned, experimental data for the breakage function are often reported as $B_M(v,w)$ in the literature. They can be easily converted to $b_M(v,w)$ by using the differential form of Eq. 4 and then to $b(v,w)$ by using Eq. 11. Three functional forms for the number-based breakage function are considered in this study:

1. *A uniform breakage function model.* It assumes that when a particle breaks, it has an equal chance of forming a particle of any smaller size.
2. *A parabolic breakage function model.* This model implies that when a particle breaks up, it is either more or less likely to result in two child particles of very different sizes. This can be used to model a breakage process where attrition or abrasion dominates (Bemrose and Bridgwater, 1987).
3. *An empirical breakage function model.* An empirical expression for the cumulative mass breakage function has been proposed by Austin et al. (1976). It provides a good fit to the data for a wide variety of materials but has a flaw, which will be discussed below.

A New Method for Discretizing the Breakage Equation

A systematic method for the discretization of the number-based breakage equation is now presented for various expressions of the specific rate of breakage and the breakage function. For all cases, the discretized breakage PBE should cor-

rectly predict the total number of particles at all times and conserve mass. The essence of our method is to introduce and formulate probability functions, one for each case, which can properly account for the intrainterval interactions. The new breakage equation is of the form:

$$\frac{d}{dt}N_i = \sum_{j=i+1}^{\infty} \beta_j b_{ij} S_j N_j - \delta_i S_i N_i, \tag{25}$$

where the birth and death term factors, β_j and δ_i, are the probability functions added to the original PBE, Eq. 14.

To provide maximum flexibility to the user, our method allows discretization of the PSD with a constant interval size or a geometric progression of successively larger interval sizes related by a constant geometric ratio, r; that is,

$$r = \frac{v_{i+1}}{v_i} \tag{26}$$

for all i greater than zero. To approximate Eqs. 22 and 23 for discretized equations, the specific rate of breakage is defined as

$$S_1 = 0 \tag{27}$$

and

$$S_i = S_c \bar{v}_i^{\alpha} \tag{28}$$

for all i greater than 1. Thus, v_1 is chosen to be equal to the critical size below which further breakage ceases.

To determine β_j and δ_i, expressions for b_{ij} and S_i are substituted into Eq. 25. The resulting equation is summed with respect to i to obtain moment equations. Then, the time derivatives of the zeroth and first moments of the discretized equation are equated to the corresponding moments of the continuous equation using Eqs. 9 and 19. For all batch processes of crushing and grinding, mass is conserved. Therefore, the time derivative of the first moment is zero. We can take advantage of this fact to derive a general result that holds for all forms of the breakage function, b_{ij}. Substituting Eq. 25 into Eq. 20, we obtain

$$\frac{d}{dt}m_1 = \sum_{i=1}^{\infty} \bar{v}_i \sum_{j=i+1}^{\infty} \beta_j b_{ij} S_j N_j - \sum_{i=1}^{\infty} \bar{v}_i \delta_i S_i N_i. \tag{29}$$

The order of summation in a double sum can be exchanged using the following formula:

$$\sum_{i=1}^{\infty} \bar{v}_i N_i \sum_{j=i+1}^{\infty} N_j = \sum_{i=1}^{\infty} N_i \sum_{j=1}^{i-1} \bar{v}_j N_j. \tag{30}$$

Applying Eq. 30 to Eq. 29, we get

$$\frac{d}{dt}m_1 = \sum_{i=1}^{\infty} S_i N_i \left(\beta_i \sum_{j=1}^{i-1} \bar{v}_j b_{ji} - \bar{v}_i \delta_i \right). \tag{31}$$

Equating this expression to zero yields

$$\delta_i = \frac{\beta_i}{\bar{v}_i} \sum_{j=1}^{i-1} \bar{v}_j b_{ji}. \tag{32}$$

Another general result can be obtained for binary breakage. Substituting Eq. 9 into Eq. 19, we obtain

$$\frac{d}{dt}m_0 = \int_0^{\infty} \int_v^{\infty} b(v,w) S(w) n(w)\, dw\, dv - \int_0^{\infty} S(v) n(v)\, dv. \tag{33}$$

The analog of Eq. 30 is

$$\int_0^{\infty} v n(v) \int_v^{\infty} n(w)\, dw\, dv = \int_0^{\infty} n(v) \int_0^{v} w n(w)\, dw\, dv. \tag{34}$$

Applying Eq. 34 to Eq. 33, we get

$$\frac{d}{dt}m_0 = \int_0^{\infty} S(v) n(v) \int_0^{v} b(w,v)\, dw\, dv - \int_0^{\infty} S(v) n(v)\, dv. \tag{35}$$

Substitution of Eq. 12 for $m = 2$ into Eq. 35 yields the time derivative of the zeroth moment for the continuous PBE, which holds for all functional forms of $b(v,w)$ for binary breakage:

$$\frac{d}{dt}m_0 = \int_0^{\infty} S(v) n(v)\, dv. \tag{36}$$

Substituting Eqs. 22 and 23 into Eq. 36, we get

$$\frac{d}{dt}m_0 = S_c(m_{\alpha} - \overline{v_1^{\alpha}} N_1) \tag{37}$$

after applying the mean value theorem. Here, $\overline{v_1^{\alpha}}$ is the mean value of v^{α} over the size range from zero to v_1.

Model Derivations and Results

The probability functions β_j and δ_j in Eq. 25 for each of the three breakage distribution functions are derived below. Also presented are simulation results to illustrate the improvements provided by the new method.

Case I: Uniform breakage function model

Since it is equally likely to from a child particle of any given size, the number-based breakage function is independent of v and is given by

$$b(v,w) = \frac{2}{w}. \tag{38}$$

Note that it satisfies both Eqs. 12 and 13 and that the corresponding expression for $b_M(v,w)$ satisfies Eq. 3. Using Eq.

16, $B(v,w)$ can be calculated to be $2v/w$. Substitution of this result into Eq. 15 yields the following for $i < j$:

$$b_{ij} = 2\frac{v_i - v_{i-1}}{v_{j-1}}. \tag{39}$$

Case Ia: Geometric-Size Intervals with r = 2. The factors β_i and δ_i are determined as follows. One relation between β_i and δ_i can be obtained from Eq. 32 which, for a uniform breakage function and $r = 2$, becomes

$$\frac{2}{3}\beta = \delta. \tag{40}$$

Since this result is independent of the size interval under consideration, the subscripts for β_i and δ_i have been dropped. Another relation can be formed by combining Eqs. 20, 25, and 39 to get

$$\frac{d}{dt}m_0 = 2S_c\beta\sum_{i=2}^{\infty}\frac{\bar{v}_i^{\alpha}N_i}{v_{i-1}}\sum_{j=1}^{i-1}(v_j - v_{j-1}) - S_c\delta\sum_{i=2}^{\infty}\bar{v}_i^{\alpha}N_i. \tag{41}$$

Since $v_0 = 0$, we can simplify Eq. 41 as follows:

$$\frac{d}{dt}m_0 = 2S_c\beta\sum_{i=2}^{\infty}\frac{\bar{v}_i^{\alpha}N_i}{v_{i-1}}v_{i-1} - S_c\delta\sum_{i=1}^{\infty}\bar{v}_i^{\alpha}N_i + S_c\delta\bar{v}_1^{\alpha}N_1. \tag{42}$$

After further simplifications, Eq. 42 becomes

$$\frac{d}{dt}m_0 = S_c\sum_{i=1}^{\infty}(2\beta - \delta)\bar{v}_i^{\alpha}N_i - S_c(2\beta - \delta)\bar{v}_1^{\alpha}N_1. \tag{43}$$

Further rearrangements yield the result for the zeroth moment of the discretized PBE:

$$\frac{d}{dt}m_0 = (2\beta - \delta)S_c(m_{\alpha} - \bar{v}_1^{\alpha}N_1). \tag{44}$$

Comparison of Eqs. 37 and 44 shows that, if $\alpha = 0$, we have

$$2\beta - \delta = 1. \tag{45}$$

If $\alpha \neq 0$, Eq. 45 is approximately valid if $\overline{v_1^{\alpha}} \approx \bar{v}_1^{\alpha}$, or if $m_{\alpha} \gg \overline{v_1^{\alpha}}N_1$ and $m_{\alpha} \gg \bar{v}_1^{\alpha}N_1$. Note that the geometric ratio is not specified in the derivation of Eq. 45; it is applicable for any r. Solution of Eqs. 40 and 45 leads to $\beta = 3/4$ and $\delta = 1/2$. Thus, the new breakage equation (Eq. 25) becomes

$$\frac{d}{dt}N_i = \frac{3}{4}\sum_{j=i+1}^{\infty}\left(2\frac{v_i - v_{i-1}}{v_{j-1}}\right)S_jN_j - \frac{1}{2}S_iN_i. \tag{46}$$

In retrospect, we should have anticipated 3/4 and 1/2 based on probability arguments. The last term in Eq. 25, $\delta_i S_i N_i$, accounts for the disappearance of particles from interval i. If all of the child particles fall into smaller size intervals, then the number of particles removed from interval i is S_iN_i, and δ_i is equal to one. Since the number of particles removed cannot be greater than the number of parent particles, the maximum value of δ_i is one. In actuality, when S_iN_i particles are broken, $b_{ii}S_iN_i$ particles are returned to the interval. Therefore, the net number of particles removed from interval i is $(1 - b_{ii})S_iN_i$ and δ_i in Eq. 25 is equal to $(1 - b_{ii})$.

The first term in Eq. 25 accounts for birth by breakage from larger size intervals. For binary breakage, two child particles are formed from each parent particle. If $b_{jj}S_jN_j$ child particles fall back into interval j due to breakage of a parent particle in interval j, then $(2 - b_{jj})S_jN_j$ child particles fall into the intervals smaller than j, that is, 1, 2, . . . , $(j-1)$. This implies that

$$(2 - b_{jj})S_jN_j = \sum_{i=1}^{j-1}\beta_j b_{ij}S_jN_j. \tag{47}$$

Because of Eq. 17, clearly, $\beta_j = (2 - b_{jj})/2$. In other words, Eq. 17 does not account for the intrainterval interactions in that it sums only up to $(j-1)$. This is corrected by modifying b_{ij} with a birth term β_j such that

$$\sum_{i=1}^{j-1}\beta_j b_{ij} + b_{jj} = 2. \tag{48}$$

In uniform binary breakage, if a particle of size v_j is broken, the probability that a child particle falls back into interval j, b_{jj}, is equal to $(v_j - v_{j-1})/v_j$. For geometric size intervals with a ratio of 2, the range for interval j is equal to the combined range of all preceding intervals 1 to $(j-1)$. Therefore, b_{jj} is 1/2 for a uniform breakage function and this leads to $\beta = 3/4$ and $\delta = 1/2$ for all j.

As mentioned, Eq. 15, which is an assumed relation, was used in the derivation of Eq. 46. If a different, reasonable relation is assumed, for example,

$$b_{ij} = [B(v_i, v_j) - B(v_{i-1}, v_j)], \tag{49}$$

it can be shown that Eq. 46 remains unchanged.

For Case Ia, an analytical solution to the continuous mass-based breakage equation (Eq. 2) has been suggested (Prasher, 1987). The improvements of the new discretized breakage equation (Eq. 46) over the conventional discretized breakage equation (Eq. 14) in predicting the PSD are demonstrated by comparison with this exact solution, which is summarized below.

We begin by defining a quantity $R(v,t)$, which is the total mass of particles of size v or larger at time t:

$$R(v,t) = \int_v^{\infty} M(w,t)\,dw \tag{50}$$

If $S(v)$ and $B(v,w)$ have the following forms:

$$S(v) = S_c g(v) \tag{51}$$

and

$$B_M(v,w) = B'\frac{g(v)}{g(w)}, \tag{52}$$

then Eq. 2 can be transformed to the following equation in terms of $R(v,t)$. Here, $g(v)$ is a nondecreasing monotonic function in v and B' is a constant:

$$\frac{dR(v,t)}{dt} = -S_c g(v) R(v,t). \tag{53}$$

The solution of Eq. 53 is

$$R(v,t) = R(v,0)\exp(-S_c g(v)t). \tag{54}$$

Clearly, Eq. 54 is applicable to Case Ia for $\alpha = 2$. Using Eqs. 4, 11, and 38 we can show that $B_M(v,w) = v^2/w^2$. Thus, $g(v) = v^2$ and $B' = 1$.

An analytical expression for the number of particles in interval i can be derived from Eqs. 50 and 54:

$$N_i = -\frac{1}{\rho}\int_{v_{i-1}}^{v_i} \frac{1}{v}\left(\frac{\partial R(v,t)}{\partial v}\right) dv. \tag{55}$$

If the particles are initially distributed evenly across the top size interval, Eq. 55 can be simplified to

$$N_i = \frac{\sqrt{\pi S_c t}}{\rho} M_T\left[\mathrm{erf}\left(v_i\sqrt{S_c t}\right) - \mathrm{erf}\left(v_{i-1}\sqrt{S_c t}\right)\right], \tag{56}$$

where M_T is the total mass in the system. This solution assumes that the specific rate of breakage S_1 is not equal to zero.

For these simulations, the breakage rate constant S_c is 5×10^{-12} min^{-1}, the breakage rate exponential factor α is 2, the density is 3.217 g/cm^3, which is the density of SiC, and the breakage function is uniform. An initial charge of 10 kg of spherical particles is evenly distributed with respect to volume and is in the top size range between 707 and 841 μm in diameter. Twenty (20) size intervals are used. The critical size v_1 is 594 μm^3 in volume or 10.43 μm in diameter.

Simulation results for the zeroth moment as a function of time for the new discretized breakage equation (Eq. 46), the conventional discretized equation (Eq. 5), and the analytical solution (Eq. 56) are shown in Figures 2a and 2b. The fourth-order Runge-Kutta technique is used for integrating the discretized equations. Clearly, the new discretized equation is much closer to the continuous equation results, and the conventional equation generates too many particles in the first hour (Figure 2a) as well as in the extreme case where the simulation runs for 60,000 min (Figure 2b).

That the new discretized PBE predictions differ slightly from the analytical solution to the continuous equation is not unexpected. First, the analytical solution assumes that all particles continue to break as grinding progresses, but the discretized equation assumes that particles smaller than the critical size, v_1, do not break. Second, the match between Eqs. 37 and 44 is exact only when m_α is the same and when $\overline{v_1^\alpha}$ in Eq. 37 equals $\bar{v}_1^\alpha$ in Eq. 44. Note that m_α in Eqs. 37 and 44 is defined by Eqs. 19 and 20, respectively. Since these matches are rarely exact, there is always a discrepancy between the discretized and continuous equations.

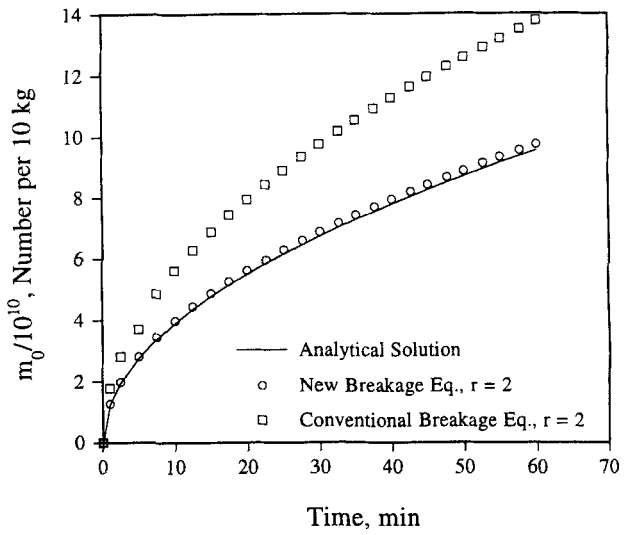

Figure 2a. Zeroth moment vs. time for 60 min for a uniform breakage function.

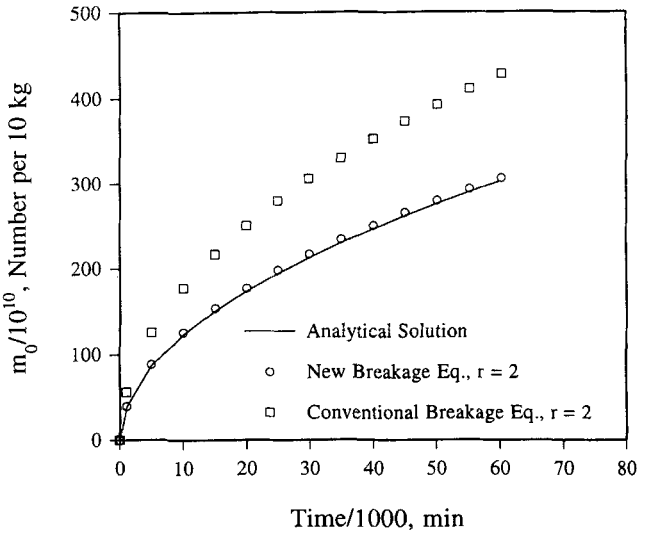

Figure 2b. Zeroth moment vs. time for 60,000 min for a uniform breakage function.

One question that arises is how sensitive the simulation is to the choice of v_1 or the number of size intervals used. This is tested by running the simulation with 10, 15, and 20 size intervals. Each simulation uses a geometric size interval ratio of two and has an initial charge of 10 kg of particles in the size range between 707 and 841 μm in diameter. Since the same geometric ratio and maximum particle size is used in each simulation, the nine largest size intervals are the same in all three cases. The exception is v_1, which increases as the number of size intervals decreases.

As shown in Figure 3, the simulations predict the same results for 15 or more intervals but yield a large error when only 10 intervals are used. A detailed review of the simulation data provides the reasons. After grinding for 0.5 min, there are very few particles in the seven largest size intervals.

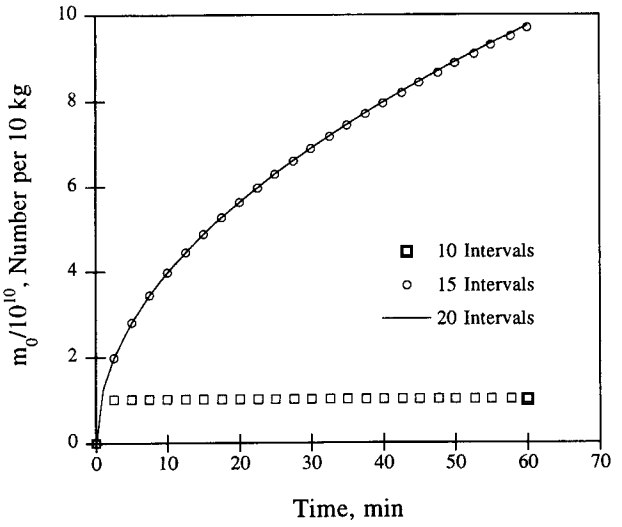

Figure 3. Zeroth moment as a function of time based on 10, 15 and 20 size intervals for a uniform breakage function.

For a simulation with 15 or more intervals, less than 1 percent of the particle mass is in the first interval. For the simulation with 10 size intervals, over 50 percent of the particle mass is in the first interval. Since particles in the first interval no longer break, the total number of particles increases very slowly from this point on. This underscores the significance of using a sufficiently small v_1 if its exact value is not known.

Although the new discretized equation is developed to predict the correct total number of particles, it is not guaranteed to give the correct PSD is general. To compare results, PSDs at 0.5, 5, and 59.6 min are shown in Figures 4a, 4b, and 4c, respectively, for the new and conventional discretized equations and the continuous equation. The new discretized equation is much more accurate than the conventional discretized equation at predicting the PSD. This is obviously a side benefit of predicting the correct total number of particles.

Plotting the mass remaining in the largest (20th) size interval as a function of time indicates the rate of breakage. Without child particles generated due to breakage of larger parent particles, the data should form a straight line on a semilog graph, with the slope indicating the rate of breakage. As shown in Figure 5, the rate of breakage for the conventional discretized equation is much higher than for the continuous and new discretized equations. This demonstrates the significance of the death term factor δ_i in the new discretized equation. The corrected specific rate of breakage of the new equation matches the specific rate in the continuous equation.

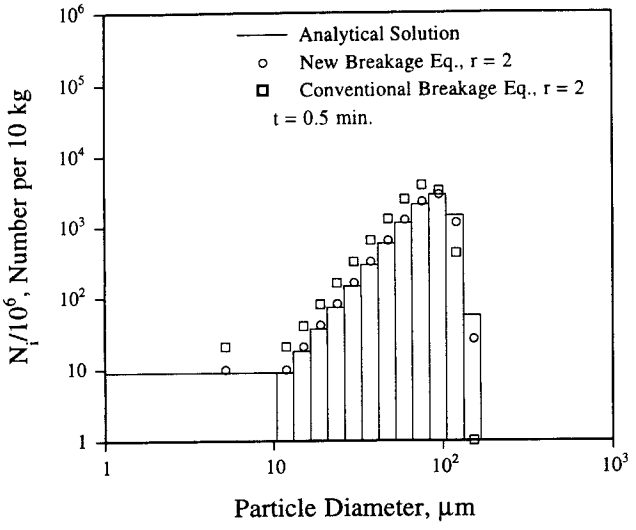

Figure 4a. PSDs calculated with the continuous, new and conventional discretized equations for a uniform breakage function at 0.5 min.

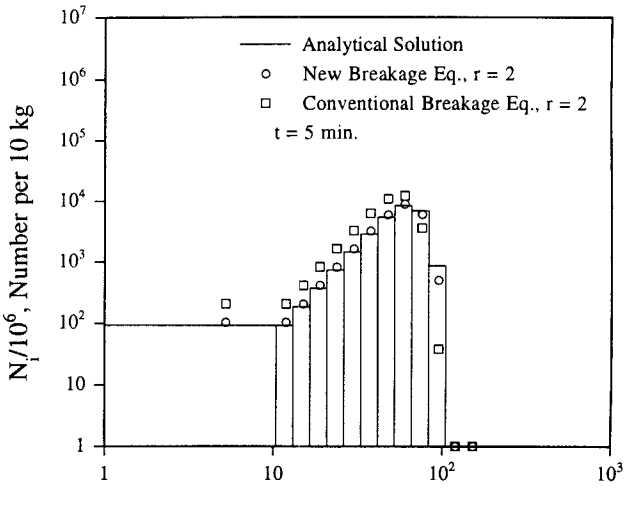

Figure 4b. PSDs at 5 min.

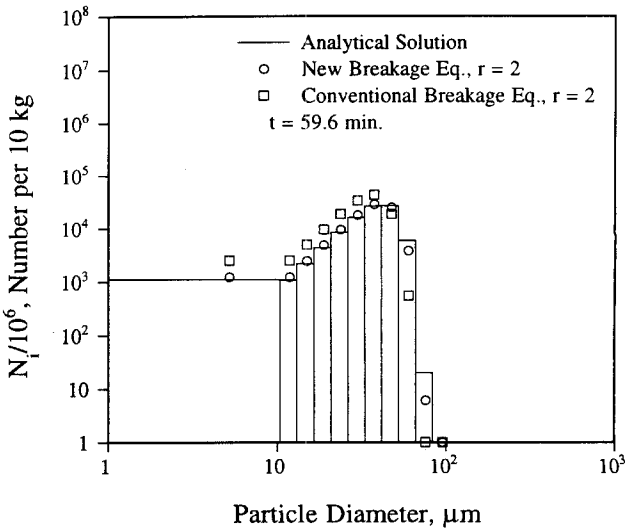

Figure 4c. PSDs at 59.6 min.

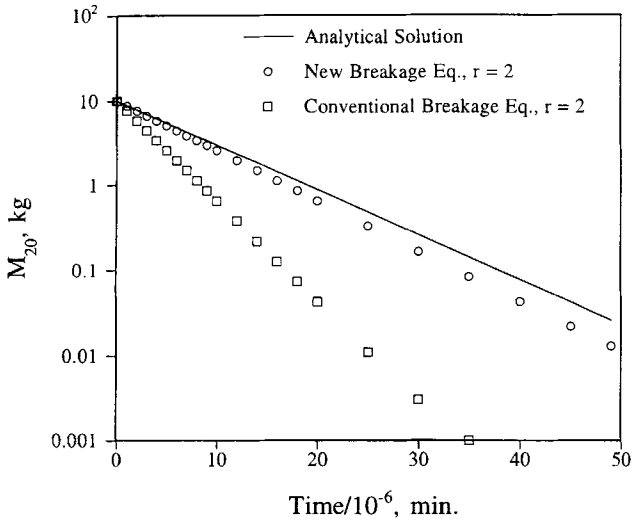

Figure 5. Mass in the highest size interval, M_{20}, vs. time for a uniform breakage function.

Case Ib: Geometric-Size Intervals with $r > 1$. Although the preceding development is based on a geometric-size ratio of two, this may be generalized for any value of r greater than 1. For uniform breakage, Eq. 32 simplifies to

$$\delta = \beta\left(\frac{2}{r+1}\right). \tag{57}$$

Solving Eqs. 45 and 57 for a generalized discretized equation with a geometric ratio of r, we obtain for the values of β and δ

$$\beta = \frac{r+1}{2r} \tag{58}$$

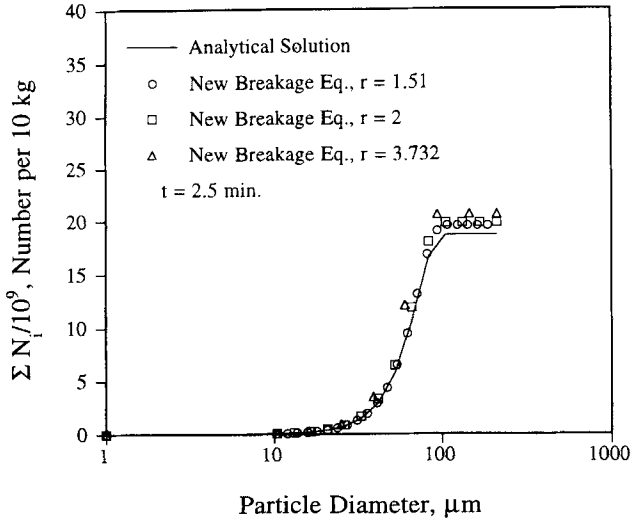

Figure 6. Effect of geometric ratio on the cumulative particle size distribution at 2.5 min for a uniform breakage function.

and

$$\delta = \frac{1}{r}. \tag{59}$$

As in Case Ia, these expressions are good for a constant rate of breakage or for the size-dependent rate of breakage.

Simulation results for discretized equations should not change with the geometric ratio used in setting up size intervals. In Figure 6, the cumulative number distribution after 2.5 min of breakage shows that there is little difference for r ranging from 1.51 to 3.732. The data are, for reasons discussed previously for Figures 2a and 2b, slightly different from the analytical results.

Case Ic: Equal-Size Intervals. Equal-size intervals are preferred to geometric-size ratios if the expected PSD does not have a long tail for large sizes. In this case, the factors β_i and δ_i change with the interval. From Eq. 32, it can be shown that

$$\delta_i = \frac{2\beta_i v_{i-1}}{v_i + v_{i-1}}. \tag{60}$$

Following the same procedure for the zeroth moment for Case Ia, we get

$$2\beta_i - \delta_i = 1. \tag{61}$$

Solving Eqs. 60 and 61 yields

$$\beta_i = \frac{v_i + v_{i-1}}{2v_i} \tag{62}$$

and

$$\delta_i = \frac{v_{i-1}}{v_i}. \tag{63}$$

Equations 62 and 63 are also applicable to geometric-size intervals. For $i > 1$, Eqs. 58 and 59 can be recovered by substituting r, as defined in Eq. 26, into Eqs. 62 and 63. For equal intervals, v_i is related to v_1 by

$$v_i = iv_1. \tag{64}$$

Combining Eqs. 25, 39, 62, 63 and 64 yields the following discretized equation for equal intervals:

$$\frac{d}{dt}N_i = \sum_{j=i+1}^{\infty} \frac{2j-1}{j(j-1)} S_j N_j - \frac{i-1}{i} S_i N_i. \tag{65}$$

This equation conserves mass and correctly predicts the number of particles formed by breakage. In addition, this equation is good for a constant rate of breakage or for the size-dependent rate of breakage.

Simulations for 20 equal-size intervals are based on the same particle density and breakage rate as those for the geometric-size intervals. An initial 10 kg charge is evenly distributed with respect to volume in the top size interval be-

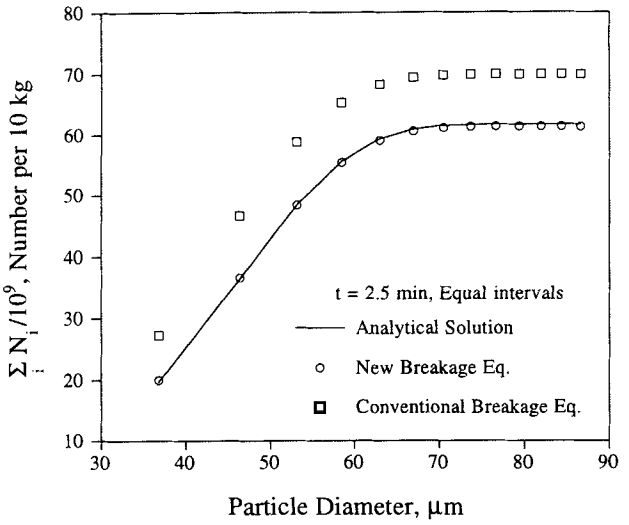

Figure 7. Comparison of the continuous, new and conventional discretized equations for equal intervals at 2.5 min for a uniform breakage function.

tween 98.3 and 100 μm. The critical size v_1 is 36.8 μm in diameter. As shown in Figure 7, the results for the new discretized equation and the analytical solution are nearly identical, but the conventional discretized equation overestimates the number of particles in the smaller intervals.

Case II: Parabolic breakage function model

We show below a general derivation for geometric-size intervals with $r > 1$. A number breakage function that conserves mass, is symmetric, and represents binary breakage is

$$b(v,w) = \frac{24\left(1-\frac{hw}{2}\right)\left(v^2 - vw + \frac{w^2}{4}\right)}{w^3} + h. \quad (66)$$

The first term on the RHS of Eq. 66 equals zero for $v = w/2$. Thus, h is the probability that a parent particle breaks into two equal-sized child particles. To be physically plausible, $b(v,w)$ must have nonnegative values for all v and w, where $v < w$. Therefore, h must be greater than or equal to zero and less than or equal to $3/w$. When h is less than (greater than) $2/w$, the parabola is concave (convex). When h is $2/w$, the equation simplifies to the case of uniform breakage. The cumulative breakage function for Eq. 66 is

$$B(v,w) = \left(1-\frac{hw}{2}\right)\left(8\frac{v^3}{w^3} - 12\frac{v^2}{w^2} + 6\frac{v}{w}\right) + hv. \quad (67)$$

The discretized breakage function is derived from the cumulative breakage function using Eq. 15:

$$b_{ij} = \left(1-\frac{hv_{j-1}}{2}\right)\left(\frac{8(v_i^3 - v_{i-1}^3)}{v_{j-1}^3} - \frac{12(v_i^2 - v_{i-1}^2)}{v_{j-1}^2} + \frac{6(v_i - v_{i-1})}{v_{j-1}}\right) + h(v_i - v_{i-1}). \quad (68)$$

Following the same procedure for the uniform breakage model, we get for the zeroth moment

$$\frac{d}{dt}m_0 = \sum_{i=1}^{\infty} \beta_i \left(2 - \frac{1}{\bar{v}_i}\sum_{j=1}^{i-1} \bar{v}_j b_{ji}\right) S_i N_i. \quad (69)$$

It can readily be shown that

$$\sum_{i=2}^{\infty} S_i N_i = S_c(m_\alpha - \bar{v}_1^\alpha N_1). \quad (70)$$

Comparing Eqs. 37, 69, and 70 shows that β_i is

$$\beta_i = \frac{1}{\left(2 - \frac{1}{\bar{v}_i}\sum_{j=1}^{i-1} \bar{v}_j b_{ji}\right)}. \quad (71)$$

Then, δ_i can be obtained by substituting Eq. 71 into 32:

$$\delta_i = \frac{\frac{1}{\bar{v}_i}\sum_{j=1}^{i-1} \bar{v}_j b_{ji}}{2 - \frac{1}{\bar{v}_i}\sum_{j=1}^{i-1} \bar{v}_j b_{ji}}. \quad (72)$$

A new discretized equation with Eqs. 71 and 72 applies to both geometric- and equal-size intervals.

Since no analytical solution is available for this case, comparisons are made for the case where $h = 0$ in Eq. 66 between the new and the conventional discretized equations only. The simulation input data as well as the initial PSD are the same as in Case Ia. Figure 8 shows the zeroth moment as a function of time. The conventional equation breaks the particles more quickly than the new discretized equation. Both the conventional and new discretized equations conserved mass during the simulation.

Case III: Empirical breakage function model

To ensure that the procedure used for developing the new discretized equations is applicable for real materials, it is important to consider experimental breakage distribution functions. Such an expression was proposed by Austin et al. (1976), which was found to provide a good fit to the data for a wide range of materials:

$$B_M(v,w) = \phi\left(\frac{v}{w}\right)^{\gamma/3} + (1-\phi)\left(\frac{v}{w}\right)^{\beta'/3} \quad (73)$$

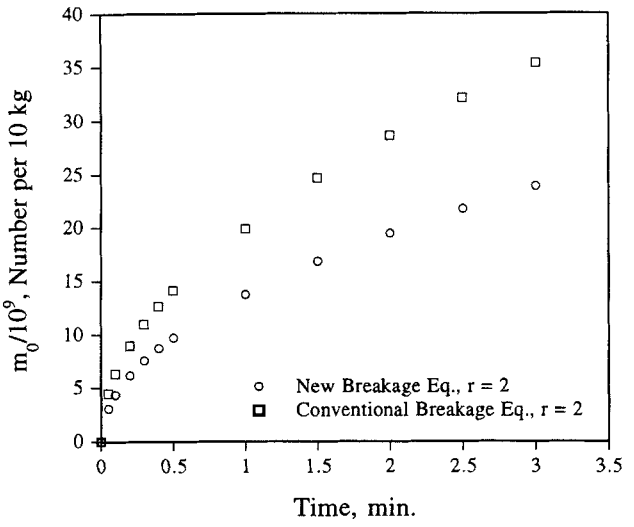

Figure 8. Zeroth moment vs. time for a parabolic breakage function.

Here, γ, β', and ϕ are parameters used to fit the experimental data. These parameters vary with the material being ground and the type of crushing mill. For materials such as SiC, quartz, cement clinker, and limestone, γ ranges from 0.59 to 1.17, β' ranges from 3.2 to 4.7, and ϕ ranges from 0.2 to 0.36. Taking the derivative of the cumulative mass breakage function and multiplying the result by w/v produces the following number breakage function:

$$b(v,w)=\frac{\phi\gamma}{3w}\left(\frac{v}{w}\right)^{(\gamma/3)-2}+\frac{(1-\phi)\beta'}{3w}\left(\frac{v}{w}\right)^{(\beta'/3)-2}. \quad (74)$$

Unlike the parabolic and uniform breakage function models, this model is not a binary breakage model. This can be seen by observing that Eq. 74 is not symmetric or by substituting Eq. 74 into Eq. 12 to show that the number of child particles m depends on the values of ϕ, γ, and β'. As just mentioned, γ is on the order of unity. Therefore, the first term on the RHS of Eq. 74 is unbounded when the particle volume v is sufficiently small. Thus, this expression predicts that an infinite number of small particles is produced, which is physically unrealistic. This problem is akin to the "shattering" transition in which a fraction of the mass of the system is lost to form a new phase of zero-sized particles (McGrady and Ziff, 1987).

In crushing and grinding practice, it is known that particles below a limiting size are not produced (Kendall, 1978; Perry et al., 1984). Therefore, we can correct the infinite number of particles problem by applying a limiting size to the empirical number breakage function. This smallest possible particle size, σ, varies with the material being ground and the equipment used for grinding.

The previous zeroth-moment derivation, Eq. 37, intended for binary breakage, is no longer valid. A similar expression is derived as before by substituting the number breakage function, Eq. 74, into an alternate form of the continuous size PBE (Eq. 33), which accounts for the limiting size assumption:

$$\frac{d}{dt}m_0=\int_\sigma^\infty\int_v^\infty b(v,w)S(w)n(w)\,dw\,dv-\int_\sigma^\infty S(v)n(v)\,dv. \quad (75)$$

In essence, particles smaller than σ are eliminated by truncation. Substituting Eq. 74 into Eq. 75, we obtain after a few algebraic manipulations

$$\frac{d}{dt}m_0=S_c\left[\frac{\phi\gamma}{\gamma-3}+\frac{(1-\phi)\beta'}{\beta'-3}-1\right](m_\alpha-\bar{v}_1^\alpha N_1)$$
$$-S_c\sigma^{c_1}\left(\frac{\phi\gamma}{\gamma-3}\right)(m_{c_2}-\bar{v}_1^{c_2}N_1)$$
$$-S_c\sigma^{c_3}\left(\frac{(1-\phi)\beta'}{\beta'-3}\right)(m_{c_4}-\bar{v}_1^{c_4}N_1). \quad (76)$$

Here, c_1 ($=\gamma/3-1$), c_2 ($=\alpha-\gamma/3+1$), c_3 ($=\beta'/3-1$), and c_4 ($=\alpha-\beta'/3+1$) are constants. Using an equation similar to Eq. 75, the result for the first moment is

$$\frac{d}{dt}m_1=-S_c\left[\phi\sigma^{\gamma/3}m_{c_2}+(1-\phi)\sigma^{\beta'/3}m_{c_4}\right]. \quad (77)$$

Thus, volume is not conserved with the empirical breakage function after correcting for the problem of having infinitely many small particles. However, the change in volume approaches zero as σ approaches zero.

The discretized number breakage function is derived using the usual procedure. We substitute Eq. 74 into Eq. 16 to obtain the cumulative breakage function, $B(v,w)$, which can then be used in Eq. 15 to determine b_{ij}. For i equal to one, σ is substituted for v_0 as follows to include the limiting size assumption:

$$b_{1j}=[B(v_1,v_{j-1})-B(\sigma,v_{j-1})]. \quad (78)$$

The resulting equation is

$$b_{1j}=c_5\frac{v_1^{c_1}-\sigma^{c_1}}{v_{j-1}^{c_1}}+c_6\frac{v_1^{c_3}-\sigma^{c_3}}{v_{j-1}^{c_3}}. \quad (79)$$

For i greater than one, we have

$$b_{ij}=c_5\frac{v_1^{c_1}-v_{i-1}^{c_1}}{v_{j-1}^{c_1}}+c_6\frac{v_1^{c_3}-v_{i-1}^{c_3}}{v_{j-1}^{c_3}}. \quad (80)$$

Here, c_5 ($=\phi\gamma/(\gamma-3)$) and c_6 ($=(1-\phi)\beta'/(\beta'-3)$) are constants. Since the limiting size varies between wet and dry grinding and with the type and size of the equipment, σ must be determined experimentally.

This procedure is repeated for the discretized PBE by using Eqs. 79 and 80 for b_{ij}. Then the discretized zeroth- and first-moment equations, which are not shown here, are compared with the continuous zeroth-moment equation (Eq. 76) and set to zero, respectively, to determine β_i and δ_i in the

discretized expressions. In other words, despite Eq. 77, conservation of mass is ensured by setting the time derivative of the first moment of the discretized equation to zero. The algebra is straightforward but tedious and is not presented here. The resulting expression for β_i is

$$\beta_i = \frac{c_5 + c_6 - c_5\left(\frac{\sigma}{\bar{v}_i}\right)^{c_1} - c_6\left(\frac{\sigma}{\bar{v}_i}\right)^{c_3} - 1}{c_5 + c_6 - c_5\left(\frac{\sigma}{v_{i-1}}\right)^{c_1} - c_6\left(\frac{\sigma}{v_{i-1}}\right)^{c_3} - \frac{1}{\bar{v}_i}\sum_{j=1}^{i-1}\bar{v}_j b_{ji}}; \quad (81)$$

δ_i is obtained by substituting Eq. 87 into Eq. 32 to obtain

$$\delta_i = \frac{\left[c_5 + c_6 - c_5\left(\frac{\sigma}{\bar{v}_i}\right)^{c_1} - c_6\left(\frac{\sigma}{\bar{v}_i}\right)^{c_3} - 1\right]\frac{1}{\bar{v}_i}\sum_{j=1}^{i-1}\bar{v}_j b_{ji}}{c_5 + c_6 - c_5\left(\frac{\sigma}{v_{i-1}}\right)^{c_1} - c_6\left(\frac{\sigma}{v_{i-1}}\right)^{c_3} - \frac{1}{\bar{v}_i}\sum_{j=1}^{i-1}\bar{v}_j b_{ji}}. \quad (82)$$

Equations 79 to 82 are substituted into Eq. 25 to form the new discretized breakage equation. This discretized equation correctly predicts the number of particles formed by breakage and conserves mass. Equations 81 and 82 are in a general form that applies to both geometric and equal-size intervals.

Simulation results are compared with experimental data for SiC at various grinding times (Austin et al., 1976). For these simulations, the constant for the rate of breakage is 5.229×10^{-4} min^{-1}, the rate of breakage parameter α is equal to 0.347, and the density of SiC is 3.217 g/cm^3. Experimental values for γ, β', and ϕ in the empirical breakage function are 1.17, 4.0, and 0.36, respectively. The simulations are performed with an initial charge of 10 kg of particles evenly distributed with respect to volume in the size range between 707 and 841 μm in diameter. Several simulations were performed with different values of the limiting size parameter, σ, to determine a value that was consistent with the experimental data.

Experimental data in cumulative mass distribution are compared to simulation results with the diameter of the limiting size σ equal to 3.37 μm, which is smaller than the diameter of the critical size v_1 of 10.43 μm. As shown in Figure 9, there is a good agreement of simulation and experimental results for all grinding times of 0.5, 1, 3, 6, 30, and 60 min reported in the article.

Concluding Remarks

A general method is presented for developing number-based discretized breakage PBEs, which account for the intrainterval interactions. This method is applicable to a specific rate of breakage with a power law form, and to both theoretical and empirical breakage functions. In all cases, mass is conserved. For most of the cases considered, the total number of particles produced is approximately but closely predicted. The exception is Case Ia with a constant specific rate of breakage ($\alpha = 0$), where the prediction is exact. Also, the new method provides a significant improvement over the conventional discretization method in predicting the PSD. In addition, this general method allows the convenience of using

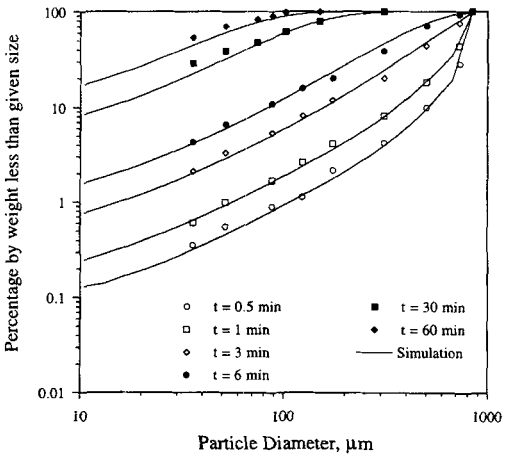

Figure 9. Comparison of experimental data with simulations for an empirical breakage function.

geometric- or equal-size intervals. Depending on the application of the breakage equation, geometric intervals may be preferred over equal intervals or vice versa.

Although we focus on a batch system in the method development, the equations formulated are also valid for a system with inflow and outflow of particles. For example, we have for a steady-state continuous crusher

$$Fn(v) = Fn_{\text{in}}(v) + V_t \rho \int_v^\infty b(v,w)S(w)n(w)\,dw - V_t \rho S(v)n(v). \quad (83)$$

Here, F is the total mass flow rate of solids in and out of the crusher, n_{in} is the PSD in the inflow, V_t is the volume of solids inside the crusher, and ρ is the solid density. The new discretized equation for Eq. 83 is

$$FN_i = FN_{i,\text{in}} + V_t \rho \sum_{j=i+1}^{\infty} \beta_j b_{ij} S_j N_j - V_t \rho \delta_i S_i N_i. \quad (84)$$

The birth and death term factors are identical to those developed for the batch system for the following reason. The time derivatives of the zeroth and first moments for the continuous equation (Eq. 9) and the new discretized equation (Eq. 25) are matched for the batch case. Clearly, the zeroth and first moments of Eqs. 83 and 84 can be matched in exactly the same manner. For the same reason, the same factors can be used for unsteady-state continuous crushers.

The new discretized PBEs are based on particle volume. An alternative is to use a characteristic length, such as particle diameter. Actually, length-based PBEs are rather common. Such a length-based breakage equation can be discretized in exactly the same manner as the volume-based equation to determine the length-based birth and death term factors. Furthermore, although the zeroth and first moments are matched in this article, the same procedure can be used to match any two moments. In that event, properties represented by these two moments are correctly predicted.

The new discretization method can be extended in a number of directions. First, it is limited to a user-specified geometric ratio for geometric-size intervals, or a specified inter-

val size for equal-size intervals. For multimodal PSDs (Popplewell and Peleg, 1992), it would be convenient to use two or more geometric ratios, or even use both geometric- and equal-size intervals, for a given particle size range. Second, the theoretical breakage functions, uniform and parabolic, are limited to binary breakage. Although the empirical breakage function is not a binary breakage model, it is fundamentally flawed. Given the recent interest in breakage with multiple child particles, developments in the basic statistics of breakage would be worthwhile efforts (Davis, 1989; Chang et al., 1991; Zhang et al., 1991; Calabrese et al., 1992). Third, in addition to the zeroth and first moments, matching of higher moments can lead to an even better prediction of the PSD. Finally, the ultimate goal of our work is to use the discretized breakage equation in the computer simulation of chemical plants with solids processing steps. To this end, we need to model breakage in equipment such as crushers, crystallizers, cyclones, fluidized-beds, and rotary-drum dryers. Efforts in these directions are under way.

Acknowledgment

The support of the National Science Foundation (Grant CTS-9211673) for this research is gratefully acknowledged.

Notation

h = height of middle of parabolic function, no./no.
x = particle diameter, μm
ω_i = mass fraction in interval i, kg/kg

Literature Cited

Austin, L., K. Shoji, V. Bhatia, V. Jindal, K. Savage, and R. Klimpel, "Some Results on the Description of Size Reduction as a Rate Process in Various Mills," *Ind. Eng. Chem. Proc. Des. Dev.*, **15**, 187 (1976).

Barton, G. W., and J. D. Perkins, "Experiences with SPEEDUP in the Mineral Processing Industries," *Chem. Eng. Res. Des.*, **66**, 408 (1988).

Bemrose, C. R., and J. Bridgwater, "A Review of Attrition and Attrition Test Methods," *Powder Technol.*, **49**, 97 (1987).

Calabrese, R. V., M. H. Wang, N. Zhang, and J. W. Gentry, "Simulation and Analysis of Breakage Phenomena," *Trans. Inst. Chem. Eng.*, **70**, Part A, 189 (1992).

Chang, Y. C., R. V. Calabrese, and J. W. Gentry, "An Algorithm for Determination of the Size-Dependent Breakage Frequency of Droplets, Flocs and Aggregates," *Part. Part. Syst. Charact.*, **8**, 315 (1991).

Cohen, E. R., and E. U. Vaughan, "Approximation Solution of the Equation for Aerosol Agglomeration," *J. Colloid Interf. Sci.*, **35**, 612 (1971).

Davis, H. T., "On the Statistics of Randomly Broken Objects," *Chem. Eng. Sci.*, **44**, 1799 (1989).

Evans, L. B., "Simulation with Respect to Solid Fluid Systems," *Comput. Chem. Eng.*, **13**, 343 (1989).

Evans, L. B., B. Joseph, and W. D. Seider, "System Structures for Process Simulation," *AIChE J.*, **23**, 658 (1977).

Gelbard, F. M., *The General Dynamic Equation for Aerosols*, PhD Thesis, California Institute of Technology, Pasadena (1979).

Goldfarb, S., J. Coon, J. Tanger, K. M. Ng, and C. F. Chu, "Crystallization Process Optimization Using PRO/II," AIChE Meeting, Chicago (1990).

Hounslow, M. J., R. L. Ryall, and V. R. Marshall, "A Discretized Population Balance for Nucleation, Growth and Aggregation," *AIChE J.*, **34**, 1821 (1988).

Hounslow, M. J., "A Discretized Population Balance for Continuous Systems at Steady State," *AIChE J.*, **36**, 106 (1990).

Hulburt, H. M., and S. Katz, "Some Problems in Particle Technology. A Statistical Mechanical Formulation," *Chem. Eng. Sci.*, **19**, 555 (1964).

Jones, G. L., "Simulating the Effects of Changing Particle Characteristics in Solids Processing," *Comput. Chem. Eng.*, **8**, 329 (1984).

Kendall, K., "The Impossibility of Comminuting Small Particles by Compression," *Nature*, **272**, 710 (1978).

McGrady, E. D., and R. M. Ziff, "'Shattering' Transition in Fragmentation," *Phys. Rev. Lett.*, **58**, 892 (Mar. 2, 1987).

McGrady, E. D., and R. M. Ziff, "Analytical Solutions to Fragmentation Equations with Flow," *AIChE J.*, **34**, 2073 (1988).

Neville, J. M., and W. D. Seider, "Coal Pretreatment—Extensions of FLOWTRAN to Model Solids-Handling Equipment," *Comput. Chem. Eng.*, **4**, 49 (1980).

Perry, R. H., D. W. Green, and J. O. Maloney, *Chemical Engineers' Handbook*, 6th ed., McGraw-Hill, New York (1984).

Popplewell, L. M., and M. Peleg, "Theoretical Kinetic Model for Particulates Disintegration Processes that Result in Bimodal Size Distributions," *Powder Tech.*, **70**, 21 (1992).

Prasher, C. L., *Crushing and Grinding Process Handbook*, Wiley, New York (1987).

Rajagopal, S., K. M. Ng, and J. M. Douglas, "Design of Solids Processes: Production of Potash," *Ind. Eng. Chem. Res.*, **27**, 2071 (1988).

Rajagopal, S., K. M. Ng, and J. M. Douglas, "A Hierarchical Procedure for the Conceptual Design of Solids Processes," *Comput. Chem. Eng.*, **16**, 675 (1992).

Ramabhadran, T. E., and J. H. Seinfeld, "Self-Preserving Theory of Particulate Systems," *Chem. Eng. Sci.*, **30**, 1019 (1975).

Ramabhadran, T. E., T. W. Peterson, and J. H. Seinfeld, "Dynamics of Aerosol Coagulation and Condensation," *AIChE J.*, **22**, 840 (1976).

Ramkrishna, D., "Solution of Population Balance Equations," *Chem. Eng. Sci.*, **26**, 1134 (1971).

Ramkrishna, D., "The Status of Population Balances," *Rev. Chem. Eng.*, **3**, 49 (1985).

Randolph, A. D., and M. A. Larson, *Theory of Particulate Processes*, 2nd ed., Academic Press, New York (1988).

Shah, B. H., D. Ramkrishna, and J. D. Borwanker, "Simulation of Particulate Systems Using the Concept of the Interval of Quiescence," *AIChE J.*, **23**, 897 (1977).

Vigil, R. D., and R. M. Ziff, "On the Stability of Coagulation-Fragmentation Population Balances," *J. Colloid Interf. Sci.*, **133**, 257 (1989).

Zhang, N., Y. C. Chang, R. V. Calabrese, and J. W. Gentry, "The Use of Fibonacci Sequences to Model Ternary Breakages," *J. Aerosol Sci.*, **22**, Suppl. 1, S223 (1991).

Ziff, R. M., "New Solutions to the Fragmentation Equation," *J. Phys. A: Math Gen.*, **24**, 2821 (1991).

Ziff, R. M., "An Explicit Solution to a Discrete Fragmentation Model," *J. Phys. A: Math Gen.*, **25**, 2569 (1992).

Ziff, R. M., and E. D. McGrady, "The Kinetics of Cluster Fragmentation and Depolymerization," *J. Phys. A: Math Gen.*, **18**, 3027 (1985).

Manuscript received Jan. 24, 1994, and revision received June 3, 1994.